Transactions, **SMiRT-26**
Berlin/Potsdam, Germany, July 10-15, 2022
Division II

Preliminary results on conducting Small-Ring Test and Small-Punch Test on the same specimen.

Aniket Joshi[1], Alex Forsey[2], Richard Moat[2], Salih Güngör[2]

[1] PhD researcher, Department of Materials, STEM, The Open University, Milton Keynes MK7 6AA, United Kingdom (aniket.joshi@open.ac.uk)
[2] Senior Lecturer, Department of Materials, STEM, The Open University, Milton Keynes MK7 6AA, United Kingdom

ABSTRACT

The Small Ring Test (SRT) was proposed by Hyde and Sun (2009) as an alternative testing methodology to analyse creep properties of miniature-sized specimens. Preliminary results by Kazakeviciute et al. (2018, 2019) show that this technique may potentially be used for tensile testing as well. The Small Punch Test (SPT) was codified in the European Code of Practice (CEN CoP) in 2007 and is another small-scale specimen test technique (CWA 15627:2007). This technique is used for creep analysis as well as fatigue and tensile testing. The CoP proposes standard disc dimensions for the SPT, which are smaller than that of a ring in SRT.

In this paper, we present the preliminary results (finite element analysis and experiments) of tensile testing (via SRT and SPT) on SS316L from a single extracted specimen, to ensure that a minimal amount of material is used for material testing. The tests are done from the single extracted specimen as well as from specimens manufactured independently for comparison. These are also compared with standard Uniaxial tensile tests for better comparison.

We find that, while the tests come with their own set of challenges, there is an appreciable agreement between all the tensile tests and these tests (SRT and SPT) can be combined for much more efficient material utilisation, which remains the ethos and driving factor behind the development of small-scale specimen testing.

INTRODUCTION

The tensile test is widely used to gain an insight into a material's basic properties, such as the elastic modulus, yield strength, and so on. This is useful in life-extension cases for critical components, especially in the nuclear industry. This testing methodology for materials has been codified into standards, with the ASTM E8/E8M (2016) standard being one of them.

While recommending the testing procedures, the ASTM standards also recommend specimen dimensions and gauge lengths that should be used for this test. Gauge length refers to the length of the specimen that should be investigated under deformation. The gauge is exclusive of the overall specimen length which can be as long as 100mm for "sub-size" specimens.

While on the other spectrum of materials testing, residual creep life tests require similar specimen dimensions for their analysis. The ASTM E139 (2018) standard is one of the numerous standards that provide specimen dimension guidelines. The specimen dimensions are similar to those suggested for tensile testing as well.

Hyde et al. (2013) succinctly outlined the need for small-scale specimen testing techniques. These can be summarised as:

1. To make effective use of limited materials, especially from irradiated samples.

2. Aid in design of new alloys for application in the nuclear industry in a cost-effective manner.
3. Extract the least amount of material possible to not tamper with structural integrity of the parent structural component.
4. Ability to work with specimens that emit lesser radioactivity due to their size.
5. Better analyse the heterogeneity in scarce areas, such as weldments.

To alleviate the need for relatively large specimens, one of the small-scale specimen tests proposed was the Small Ring Test (SRT) for residual creep life analysis by Hyde and Sun (2009). This testing methodology boasted of a high equivalent gauge length compared to other small-scale specimen tests. This testing methodology has also proven to be effective in analysing the creep behaviour of creep-resistant materials such as Nickel superalloys, as demonstrated by Hyde et al. (2013).

The test involves placing a ring-based sample (either circular or elliptical) between two loading pins and then moving one of the pins in the vertical direction. The measure of interest is the force-displacement curve that is generated at the loading pin due to the resistance of the ring to the deformation. This data cannot be directly translated to a conventional stress-strain curve due to the multiaxial deformation that the ring undergoes. Instead, FE analysis needs to be performed to obtain reference parameters which are then used to translate the data into a conventional stress-strain/creep curve.

Kazakeviciute et al. (2018) took this test further and demonstrated that it could be used to analyse the tensile properties of a material. They used aluminium alloy 7175-T7153 and recommended that further tests be done with different materials, such as steel or nickel superalloys, and recommended testing at elevated temperatures in conjunction with the development of FE models. Kazakeviciute et al. (2019) later showed results for this at various loading rates. The material didn't exhibit any strain-rate sensitivity at room temperature in uniaxial tensile tests and the same held true for the Small Ring Tensile Test (SRTT).

Rouse et al. (2020) later demonstrated the efficacy of this test with Ti-6Al-4V (grade 23) and found good repeatability across the spectrum of tests conducted by them. They use inverse analysis in conjunction with MATLAB and Abaqus to fit the material parameters to the Ramberg-Osgood model, which does seem to give satisfactory results but diverges, like the work by Kazakeviciute et al. (2018, 2019), around the yield region.

These three papers form a crucial base of a part of this work.

Another test that forms the secondary part of this work is the Small Punch Test (SPT). The SPT is based on the work of the Miniature Disk Bend Test first proposed by Manahan (1982) and has proven to be a significant advancement in the field of small-specimen testing techniques. This testing methodology has also been codified in the European Code of Practice for Small Punch Testing (CWA 15627:2007). Originally proposed as an alternative for creep testing, this methodology does form the basis for other types of small punch tests.

The Small Punch Test involves fixing a disc of diameter 8mm and thickness 0.5mm between two dies and penetrating it with a punch (tip radius 1.25mm) at the centre. 4mm of the disc is exposed for the punch, while the remaining area is used to clamp it. The die into which it is being penetrated is recommended to have a chamfer of 0.2mm. These are the recommendations from the aforementioned Code of Practice (CWA 15627:2007). The test can be performed at a Constant Force or at Constant Displacement Rate of the punch. The former is analogous to a creep test while the latter is analogous to a tensile test and is of particular interest here.

The measurement obtained from this test is the force-displacement diagram from the punch due to the resistance it encounters during the punching operation. Due to the nature of this test, it is a multiaxial state of stress in the disc as compared to the largely uniaxial state of stress that is found in a conventional stress-strain curve.

The elastic-plastic transition load can be used to determine the yield stress and the Code of Practice delineates the analytical procedure for it, alongside procedures to determine the effective fracture strain and the fracture energy.

These conversion relationships, however, remain a topic of debate. Vijayanand et al. (2020), for instance, employ inverse modelling with the help of stereo-DIC and observe distinct deformation states that may be better suited for data interpretation compared to the approaches recommended by the CoP.

Additionally, alternative methods for estimating the ultimate tensile strength and yield strength have also been proposed. One of the initial approaches was developed by Takahashi et al. (1988) to determine the ultimate tensile strength, but there has been criticism of this method as well. This is illustrated in the study by Garcia et al. (2014) which compares a host of yield strength and ultimate tensile strength conversion relationships. For the sake of standardisation and conforming to the CoP, this paper uses the methods evidenced in the CoP.

While seemingly disjointed, these two tests do have the potential to be combined.

A circular ring for the SRT typically has a thickness of 2mm, depending on the ring's diameter. The disc of the SPT, meanwhile, has a thickness of 0.5mm. At around 10mm internal diameter for the ring, the ring can be bigger in size as compared to the disc's recommended diameter of 8mm.

Thus, with precise machining, it should be possible to extract two discs from the blank space of a ring. This would allow the industry to conduct three tests from the same size as of a ring sample. Volumetrically speaking, this would be the most material efficient way to do testing, if proven feasible. Considering a uniaxial sample of dimensions 100 x 10 x 3 (in mm), this translates to 9000mm^3 in volume for 3 tests. However, considering a ring of outer diameter 12mm and thickness 2mm, one can, theoretically, perform the 3 tests from a volume of approximately 900mm^3.

The intent of this paper is to test this hypothesis by extracting 2 discs from the blank space of a ring and test these against the conventionally extracted specimens, while also contrasting them with uniaxial tests. While this study is limited in scope only to tensile tests, the hypothesis, if true, could be translated to other forms of testing, such as creep and fatigue with good confidence. A structured outline of this paper is shown in fig. 1. The material under consideration is SS316L.

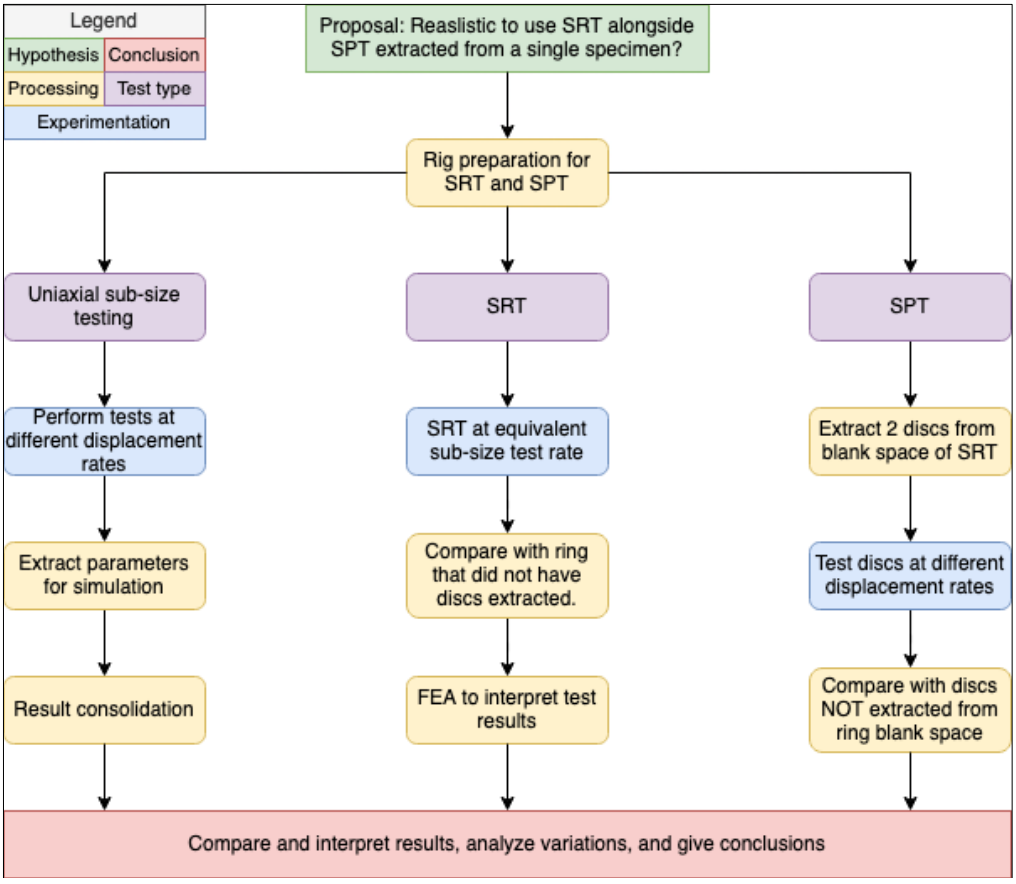

Figure 1. Outline of the paper and the research question.

METHODOLOGY

Although no strain-rate dependency has been reported for SS316L at room temperature, sub-size uniaxial tests were first carried out to analyse the same for completeness.

The parent bar was solution annealed, cold-rolled, and heat treated subsequently to 1060ºC. Micrographs were taken from the residual material between the ring and the disc, and from the parent bar as well. These are shown in fig. 2.

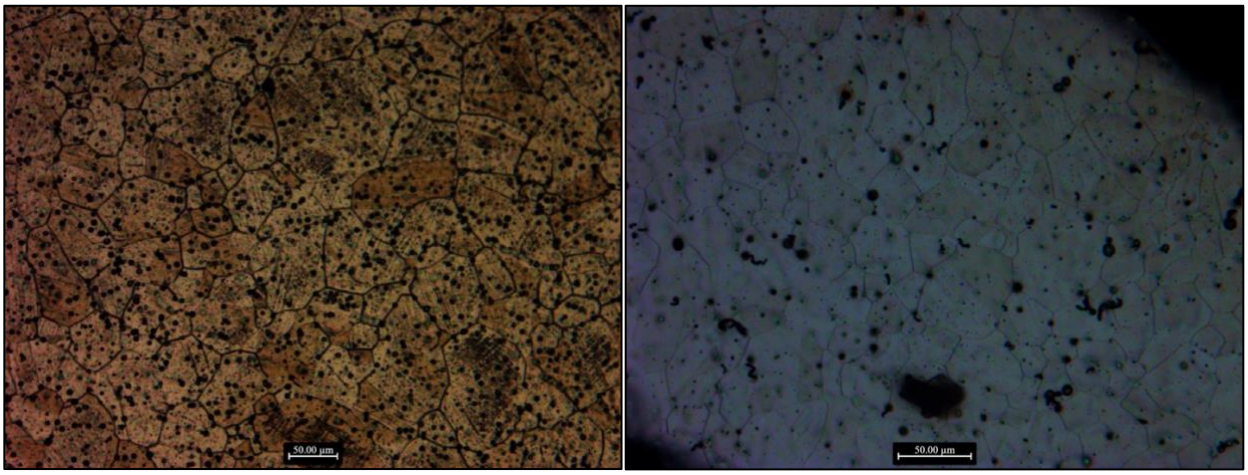

Figure 2. (left) Micrograph from the parent bar (right) Micrograph from the residual material between the ring and the disc.

The grain size was observed to be 54 µm (± 6 µm) in the parent bar and 52 µm (± 4 µm). While it is not feasible to perform grain-size measurement in the actual test samples, the residual material (the scrap between a ring's 10mm inner diameter and a disc's 8mm diameter) provides a good amount of buffer to measure this, while also allowing the capability to perform micro-hardness tests. Micro-hardness tests were performed on these samples, and the hardness was found to be in good agreement. The parent bar showed a mean hardness of 251 ± 4.36 HV, while the residual material had a hardness of 247 ± 6.41 HV.

Uniaxial tensile tests (with sub-size specimens) were performed at the loading rates of 0.1mm/min, 0.3mm/min, and 0.5mm/min. No strain-rate dependency was found.

This data was subsequently used to calculate the Poisson's ratio with the help of Digital Image Correlation (DIC) and was found to be 0.282. The stress-strain curve was averaged for all the three tests and was used to fit to the material parameters of the Ramberg Osgood model ('Deformation Plasticity' in Abaqus) for finite element analysis (FEA). The Ramberg Osgood model takes the form of:

$$\varepsilon = \frac{\sigma}{E} + \alpha\frac{\sigma}{E}\left(\frac{\sigma}{\sigma_y}\right)^{n-1}, \quad (1)$$

Where, E is the elastic modulus, ε is strain, σ_y is the yield stress, σ is the stress, while α is a constant representing the yield offset and n is the constant representing the hardening exponent. These parameters were fitted to the uniaxial data test data and were subsequently used to simulate a uniaxial test as well. The parameters obtained are shown in Table 1.

Table 1 Material parameters for the Ramberg-Osgood model, obtained from uniaxial tensile test.

Material	Displacement rate	Temperature (ºC)	Elastic Modulus (E) (GPa)	Yield Stress (σ) (MPa)	Yield offset (α)	Hardening exponent (n)

SS316L	All	Room Temperature	209.4	245	0.16224	6.85739

For the FE analysis, C3D8R element formulation was used for all the simulations. The Pin, in the SRTT, was modelled as a rigid body. The rigid body assumption was considered to reduce the computational costs. The pins for the experiments were made from Hastelloy X, and no deformation in the loading pins was observed after performing the experiments.

For the SRTT, FEA needs to be done so that the equivalent gauge lengths and gauge areas could be obtained. These take the form of:

$$L_{gauge} = \frac{\Delta L}{\varepsilon}, \tag{2}$$

$$A_{gauge} = \frac{F}{\sigma}, \tag{3}$$

Where, L_{gauge} is the equivalent gauge length, A_{gauge} is equivalent gauge section area of the ring, ΔL is the change in length, ε is the strain, F is the force on the pin, and σ is the stress.

The FEA setup of the SRTT is shown in fig. 2. Given the nature of symmetry in the ring, a 1/8th model was used to make analysis quicker. The Reference Point in the ring is shown as RP-1 and denotes the node in the middle of the ring in the experiments. A hex mesh of 0.1mm was chosen for the ring after a mesh sensitivity study, and a hex mesh 0.5mm was chosen for the sub-size test.

The loading rates used for the SRTT, along with SPTT, are summarised in Table 2, along with the relevant dimensions and source of material for the tests. The loading rate for the SPTT refers to the punch's travel rate.

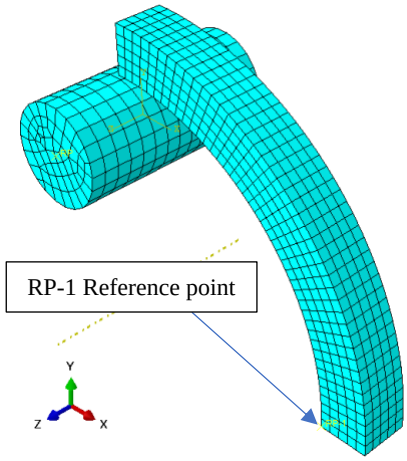

Figure 2. FEA setup of the SRTT.

Table 2. Test data with dimensions of the specimens and material history and loading rates.

Test type	Dimensions (mm)	Source of material	Loading rate (mm/min)
SRTT	Outer diameter- 13.06 Inner diameter- 10.95 Thickness- 2.015	From parent SS316L bar. Tested for comparison.	0.3
SRTT	Outer diameter- 12.05 Inner diameter- 10.01 Thickness- 2.011	From blank machined out to test the hypothesis.	0.3

SPTT	Thickness- 0.511, 0.491 Diameter- 7.98, 7.99	From parent SS316L bar. Tested for comparison.	0.1, 0.3
SPTT	Thickness- 0.509, 0.511 Diameter- 7.96, 7.97	From the blank space of a small ring test sample.	0.1, 0.3
Uniaxial sub-size	Gauge thickness- 3 Gauge height- 6 Gauge length- 50	From parent SS316L bar. Tested for comparison.	0.1, 0.3, 0.5

Two discs were extracted for the SPTT and the punch was machined as required by the Code of Practice to a radius of 1.25mm. For comparison of these discs machined (0.3mm wire for wire EDM) from the blank of the ring, 2 control tests were also performed at equivalent displacement rates. The dimensions for all the discs tested are given in Table 2.

RESULTS

Fig. 3 shows the averaged uniaxial sub-size tensile test result, alongside the Ramberg-Osgood model that was simulated to test the material parameters obtained after optimisation.

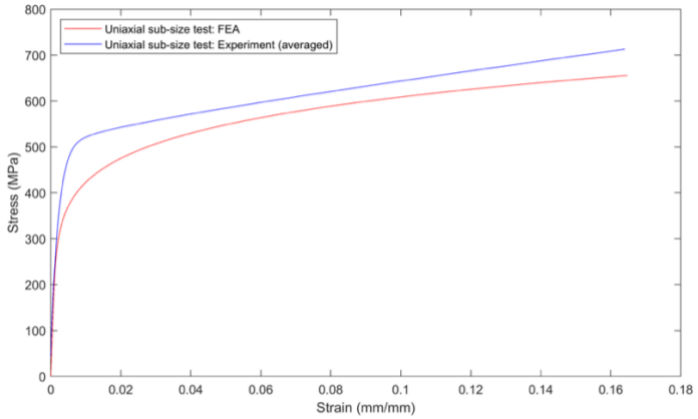

Figure 3. Averaged uniaxial sub-size test result, compared against FEA with Ramberg-Osgood model.

Fig. 4 shows the force-displacement curves obtained from the 2 SRTT and are labelled as ‘P’ for the ring from the Parent Bar, and ‘H’ for the ring that was used to test this study’s hypothesis. These are also contrasted with the FE simulations. This notation carries forward to the SPTT graphs as well, which are shown in fig. 5.

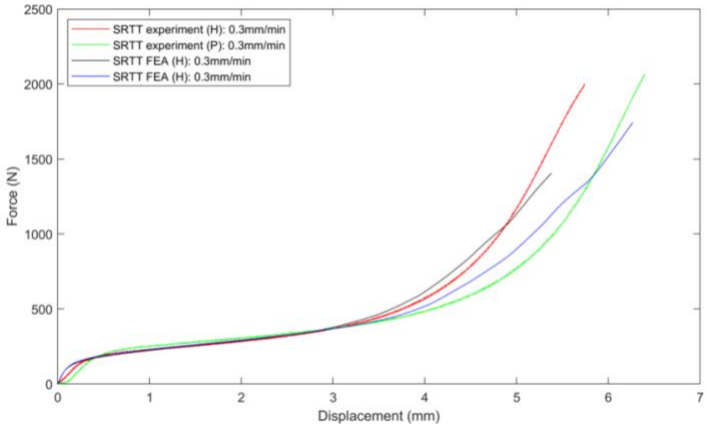

Figure 4. SRTT experiment and FEA graphs. ‘P’ represents sample from the Parent Bar while ‘H’ represents sample extracted for the hypothesis.

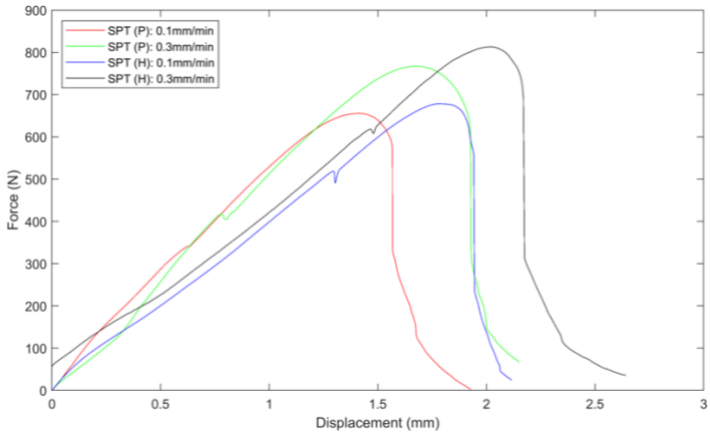

Figure 5. Force-displacement SPTT graphs from experiments.

Fig. 6 shows the equivalent gauge section area and equivalent gauge length plotted against the pin's reaction force using equation 2 and 3.

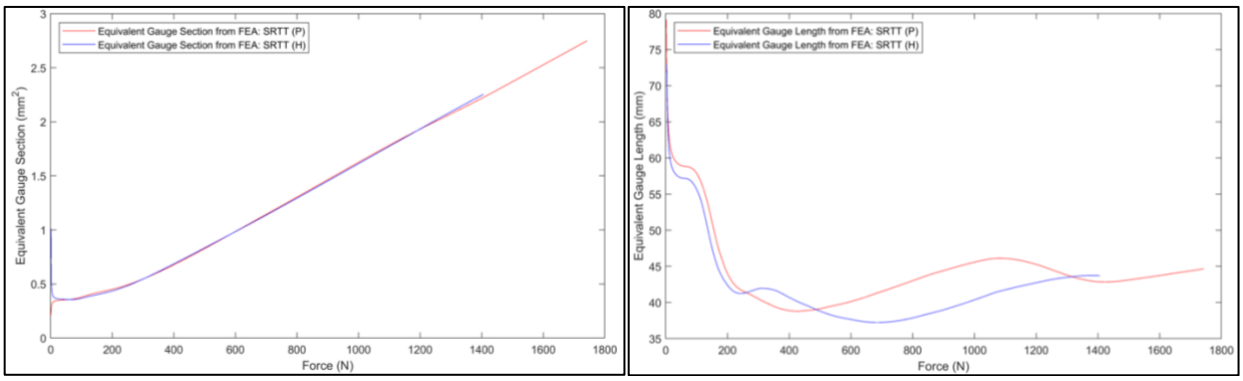

Figure 6. Evolution of Equivalent Gauge Section (left) and Equivalent Gauge Length (right) plotted with force on X-axis. These curves are then used to calculate the stress-strain curve from SRTT experiments.

Fig. 7 compares both the SRTT graphs, along with its FEA results, with the uniaxial test data.

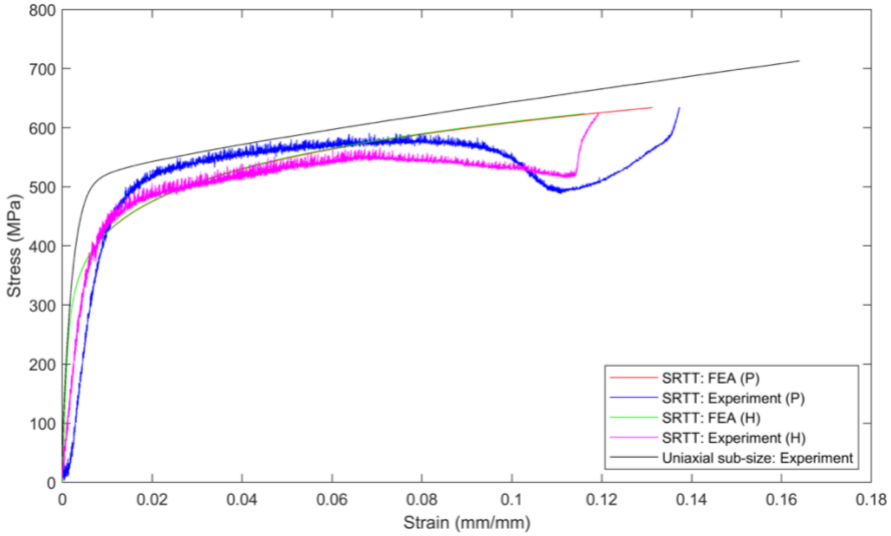

Figure 7. Stress-strain curve comparison for SRTT (experiment and FEA) and the uniaxial sub-size test.

For the SPTT, Garcia et al. (2014) summarise a variety of methods to calculate the yield stress from the small punch data. However, as mentioned previously, only the CEN (Code of Practice) method of using two tangents on the force-displacement curve is used to measure the yield stress here. The formula is given below, and the results are summarised in table 3.

$$\sigma_y = 0.476\frac{P_y}{t^2}, \tag{4}$$

Where, t is the thickness of the disc, P_y is the elastic load limit found via the two-tangent method, and σ_y is the yield stress. This relationship has been shown to be not as material dependent as other relationships, such as the one proposed by Mao and Takahashi in 1991.

Table 3. Results from all the experiments and simulations.

Test type	Loading rate (mm/min)	Source P– Parent bar H– Blank used to test the study's hypothesis F– FE simulation	Yield Stress (MPa)
Small Ring	0.3	P	277.09
Small Ring	0.3	H	275.22
Small Ring	0.3 (P), 0.3 (H)	F	202.09, 204.12
Small Punch	0.1, 0.3	P	238.84, 227.06
Small Punch	0.1, 0.3	H	312.94 347.71
Uniaxial sub-size	0.1, 0.3, 0.5	P	239, 246, 251
Uniaxial sub-size	0.3	F	245

DISCUSSIONS OF RESULTS AND CONCLUSIONS

The Ramberg-Osgood model has trouble with fitting around the yield region. This was evidenced in fig. 3 and remains a scope of improvement and has been noted in previous studies as well.

Fig. 4 showcased the force-displacement curves obtained from SRTT. Kazakeviciute et al. (2018, 2019) displace the ring by 4mm, however the ring was displaced further in this study to observe the effects of doing so. As noted by them, the nonlinearities in deformation tend to dominate and it is not of any scientific merit to take the pin to rupture.

Fig. 6 showcased the equivalent gauge section area and equivalent gauge length evolution with respect to the force experienced by the loading pin. The reaction force readings from the pin were divided by the stress at the centre of the ring (RP-1 in fig. 2) in the FE model to obtain the equivalent gauge section area. The displacement of the pin was divided by the total strain experienced at the centre of the ring as well in the FE model to obtain the equivalent gauge length.

The experimental readings of the force on the pin were divided by this equivalent gauge section area to obtain the stress and the displacement of the pin was divided by the equivalent gauge length to obtain the strain. This conversion enabled the stress-strain curves shown in fig. 7. The FE stress-strain curves of the ring, shown in fig. 7 as well, are extracted from the centre of the ring (RP-1 in fig. 2) in the FE model.

The SRTT simulation curves show a much lower yield stress value, but that can be attributed to the ill-fitting of the Ramberg-Osgood model. The experimental curves, however, are remarkably close to each other and to the reference uniaxial stress-strain curve as well. This bolsters the credibility of the hypothesis

of combining all the tests together since no significant variation is observed between ring whose blank was machined for discs, as compared to ring whose blanks was simply discarded.

The SPTT curves show a lot of variances amongst themselves as well as with respect to the other testing methodologies. This requires further investigation and lends doubt to the whole hypothesis.

However, it must also be noted that the Code of Practice formula (equation 4) is not perfect and has been criticized for its fitting. Haroush et al. (2015), who use SS316L but in thin foil discs, use the conversion factor as 0.346 instead of 0.476. Using this factor, the results change dramatically (a decrease of 27% approximately) and the yield stress values, for the discs machined out from the blanks, are more in line with the SRTT and Uniaxial sub-size tests.

Thus, it would not be prudent to discard these results based on the Code of Practice conversions alone and further investigation is strongly recommended. Further investigation should include more SPTT with discs machined from the reference parent bar and discs machined from the blank space of the SRTT samples. More punch displacement rates are also strongly recommended for further studies and advanced imaging techniques, such as the stereo-DIC methodology proposed by Vijayanand et al. (2020) would be highly beneficial.

FUTURE WORK

The study showcased the preliminary results from the hypothesis that three samples could be extracted from essentially just one SRTT sample. The results are promising and optimistic, but they also delineate the areas of improvement that can be undertaken for this material optimization technique. Further work could include:

1. Performing more SRTT at various displacement rates.
2. Performing more SPTT at various punch displacement rates and utilising various conversion factors.
3. Analysing the feasibility of DIC for SRTT to examine the strain evolution in the ring.
4. Utilising machine learning to analyse the curves generated by SRTT so that a stress-strain curve can be obtained without performing FEA.
5. Utilising data assimilation techniques for SPTT to better analyse the yield region obtained in the test's curve. As it stands currently, there is no universal analytical conversion formula for this test, and this tends to limit its usability.

All these factors are under investigation by the authors for future work, and this study forms a strong foundation for the future work being undertaken currently.

ACKNOWLEDGEMENTS

The authors are grateful to Mr. Pete Ledgard and Mr. Damian Flack for lending their manufacturing expertise throughout this whole study. Their manufacturing precision and experience helped enable this study in the first place.

REFERENCES

CWA, CEN. *15627 Workshop Agreement: Small punch test method for metallic materials*, European Committee for Standardization, Brussels (2006).

E28 Committee. (2016). *Test Methods for Tension Testing of Metallic Materials,* ASTM International. https://doi.org/10.1520/E0008_E0008M-16A

E139 Committee. (2018). *Standard Test Methods for Conducting Creep, Creep-Rupture, and Stress-Rupture Tests of Metallic Materials,* ASTM International. https://doi.org/10.1520/E0139-11R18

García, T. E., Rodríguez, C., Belzunce, F. J., & Suárez, C. (2014). "Estimation of the mechanical properties of metallic materials by means of the small punch test," *Journal of Alloys and Compounds*, *582*, 708–717. https://doi.org/10.1016/j.jallcom.2013.08.009

Haroush, S., Priel, E., Moreno, D., Busiba, A., Silverman, I., Turgeman, A., Shneck, R., & Gelbstein, Y. (2015). "Evaluation of the mechanical properties of SS-316L thin foils by small punch testing and finite element analysis," *Materials & Design*, *83*, 75–84. https://doi.org/10.1016/j.matdes.2015.05.049

Hyde, C. J., Hyde, T. H., Sun, W., Nardone, S., & De Bruycker, E. (2013). "Small ring testing of a creep resistant material," *Materials Science and Engineering: A*, *586*, 358–366. https://doi.org/10.1016/j.msea.2013.07.081

Hyde, T. H., & Sun, W. (2009). "A novel, high-sensitivity, small specimen creep test," *The Journal of Strain Analysis for Engineering Design*, *44*(3), 171–185. https://doi.org/10.1243/03093247JSA502

Hyde, T. H., Sun, W., Williams, J. A. (2013). "Requirements for and use of miniature test specimens to provide mechanical and creep properties of materials: a review," *International Materials Review: Vol 52, No 4*, 213-255. https://doi.org/10.1179/174328007X160317

Kazakeviciute, J., Rouse, J. P., De Focatiis, D. S. A., & Hyde, C. J. (2019). "The development of a novel technique for small ring specimen tensile testing," *Theoretical and Applied Fracture Mechanics*, *99*, 131–139. https://doi.org/10.1016/j.tafmec.2018.11.016

Kazakeviciute, J., Rouse, J. P., & Hyde, C. J. (2018). "The development of a novel small ring specimen tensile testing technique," *Ubiquity Proceedings*, *1*(S1), 29. https://doi.org/10.5334/uproc.29

Manahan, M. P. (1982). *The development of a miniaturized disk bend test for the determination of post-irradiation mechanical behavior* [Thesis, Massachusetts Institute of Technology]. https://dspace.mit.edu/handle/1721.1/15765

Rouse, J. P., Simonelli, M., & Hyde, C. J. (2020). "On the use of small ring testing for the characterisation of elastic and yield material property variation in additively manufactured materials," *Additive Manufacturing*, *36*, 101589. https://doi.org/10.1016/j.addma.2020.101589

Vijayanand, V. D., Mokhtarishirazabad, M., Peng, J., Wang, Y., Gorley, M., Knowles, D. M., & Mostafavi, M. (2020). "A novel methodology for estimating tensile properties in a small punch test employing in-situ DIC based deflection mapping," *Journal of Nuclear Materials*, *538*, 152260. https://doi.org/10.1016/j.jnucmat.2020.152260